Unimolecular Decomposition Pathways of Dimethyl Ether: An ab Initio Study

John J. Nash and Joseph S. Francisco*

Department of Chemistry, Purdue University, West Lafayette, Indiana 47907

Received: July 10, 1997; In Final Form: October 17, 1997[⊗]

Primary dissociation pathways have been investigated for dimethyl ether by ab initio molecular orbital methods. Reactants, transition-state structures, and products were fully optimized up to the MP2/6-311G(2df,2p) level of theory. Relative energies have been calculated with the spin-projected PMP4 and CCSD(T) post-Hartree−Fock methods using the 6-311G(2df,2p) and the expanded 6-311++G(3df,3pd) basis sets. At the CCSD-(T)/6-311++G(3df,3dp) level, the barrier height for C−O bond fission is predicted to be 81.1 kcal/mol, while that for C−H bond fission is predicted to be 93.8 kcal/mol. These theoretical results agree very well with the experimentally measured barrier heights for these two bond fission channels. However, two new primary dissociation pathways are predicted to be competitive with these bond fission processes. These findings are discussed in light of previous experimental results on dimethyl ether.

Introduction

Dimethyl ether is currently being considered as a potential fuel alternative. Critical to the development of this compound as a fuel alternative is an understanding of its combustion chemistry. Early experimental studies of dimethyl ether by Askey and Hinshelwood[1] and Leifer and Urey[2] suggested that thermal decomposition of this compound followed first-order kinetics. Benson[3] later showed that the decomposition mechanism could be explained by a chain reaction initiated by C−O bond fission (eq 1).

$$CH_3OCH_3 \rightarrow CH_3 + CH_3O \qquad (1)$$

The activation energy for the above reaction was estimated as 81.1 kcal/mol from pyrolysis experiments. In these early studies, the major decomposition products were identified as CO, CH_4, and H_2 in roughly equimolar amounts along with small amounts of CH_2O and C_2H_6.[1−3] In a later study, Benson and Jain[4] examined the stoichiometric changes of CH_2O and CH_4 as a function of temperature. During the initial stages of the reaction, the ratio of CH_2O to CH_4 was found to be about equal to 2, but this ratio increased as the reaction reached a steady state which lent additional support for a chain reaction mechanism. The formation of CH_2O and CH_4 was proposed to occur from two key steps in the reaction mechanism. First, a CH_3 radical (produced from C−O bond fission of dimethyl ether, eq 1) abstracts a hydrogen atom from a second molecule of dimethyl ether (eq 2).

$$CH_3 + CH_3OCH_3 \rightarrow CH_4 + CH_2OCH_3 \qquad (2)$$

The resulting methoxymethyl radical, CH_2OCH_3, then decomposes to fomaldehyde and methyl radical (eq 3).

$$CH_2OCH_3 + (M) \rightarrow CH_3 + CH_2O + (M) \qquad (3)$$

The net result of eqs 2 and 3 is the conversion of dimethyl ether to CH_2O and CH_4 (eq 4).

$$CH_2OCH_3 + (M) \rightarrow CH_4 + CH_2O + (M) \qquad (4)$$

On the other hand, mercury-photosensitized decomposition of dimethyl ether has been shown[5−7] to occur via an intial C−H rather than C−O bond fission process to form hydrogen atoms and methoxymethyl radical (eq 5).

$$Hg(^3P_1) + CH_3OCH_3 \rightarrow CH_3OCH_2 + H + Hg(^1S_0) \qquad (5)$$

However, the mercury-photosensitized decomposition studies of Pottie et al.[8] showed that under a high-intensity light source, 50% of the total initiation could be accounted for by the C−O bond fission process.

Infrared multiphoton decomposition studies, which typically involve dissociation on the ground-state potential energy surface, were carried out by Kutschke et al.[9] for dimethyl ether. These authors also suggested that the primary decomposition pathway for dimethyl ether involves C−O bond fission.

Due to the limited amount of experimental and theoretical work that is available for dimethyl ether, the combustion mechanism(s) for this compound are still not fully understood. Consequently, a thorough analysis of all possible decomposition processes that might compete energetically with C−H and C−O bond fission is needed. Herein, we use the results of ab initio calculations to evaluate the energetics associated with the following five decomposition reactions for dimethyl ether (eqs 6−10) and to assess whether the reactions shown in eqs 8−10 might be energetically competitive with the previously observed C−O and C−H bond fission chemistry (eqs 6 and 7, respectively).

$$CH_3OCH_3 \rightarrow CH_3O + CH_3 \qquad (6)$$

$$\rightarrow CH_3OCH_2 + H \qquad (7)$$

$$\rightarrow CH_4 + CH_2O \qquad (8)$$

$$\rightarrow CH_3OH + CH_2 \qquad (9)$$

$$\rightarrow CH_3OCH + H_2 \qquad (10)$$

Equation 8 results from a 1,3-H shift proceeding through a four-center transition state. While eq 9 results from a 1,2-H shift,

[⊗] Abstract published in *Advance ACS Abstracts,* December 1, 1997.

S1089-5639(97)02256-1 CCC: $15.00
Published on Web 01/01/1998

TABLE 1: Selected Geometrical Parameters for Reactants and Products[a]

		MP2/				
molecule	coordinate	6-31G(d)	6-311G(d,p)	6-311G(2d,2p)	6-311G(2df,2p)	exptl
H_2	HH	0.738	0.734	0.735	0.735	0.741[b]
CH_2 (C_{2v})	CH	1.109	1.110	1.102	1.102	
	HCH	102.2	101.4	101.6	101.8	
CH_3 (C_{3v})	CH	1.079	1.079	1.072	1.073	1.079[c]
	HCH	120.0	120.0	120.0	120.0	120.0
CH_4 (T_d)	CH	1.090	1.090	1.082	1.083	1.094[d]
	HCH	109.5	109.5	109.5	109.5	109.5
CH_2O (C_{2v})	CH	1.104	1.106	1.098	1.099	1.116[e]
	CO	1.221	1.210	1.209	1.206	1.208
	HCO	122.1	122.2	122.0	122.0	121.8
CH_3O (C_s)	CH′	1.101	1.102	1.094	1.096	
	CH	1.096	1.096	1.089	1.090	
	CO	1.387	1.376	1.377	1.369	
	H′CO	104.8	105.0	105.2	105.2	
	HCO	112.3	112.8	112.7	113.0	
CH_3OH (C_s)	CO	1.423	1.416	1.420	1.412	1.425[f]
	HO	0.970	0.957	0.956	0.956	0.945
	CH′	1.090	1.090	1.082	1.084	1.094
	CH	1.097	1.097	1.089	1.090	1.094
	COH	107.5	106.5	107.4	107.6	108.5
	HCO	106.3	106.9	106.7	106.9	108.3
	HCH	108.5	108.1	108.2	108.0	108.6
CH_3OCH_3 (C_{2v})	CO	1.414	1.407	1.410	1.403	1.410[g]
	CH′	1.090	1.090	1.083	1.084	1.091
	CH	1.099	1.099	1.092	1.093	1.100
	COC	111.1	110.6	110.7	110.8	111.7
	H′CO	106.9	107.3	107.5	107.7	107.2
	HCO	111.5	111.5	111.4	111.5	110.8
CH_3OCH_2 (C_1)	CO	1.425	1.418	1.420	1.413	
	C′O	1.364	1.354	1.356	1.350	
	C′H	1.088	1.088	1.080	1.080	
	C′H′	1.082	1.081	1.074	1.074	
	COC′	113.6	113.1	113.3	113.5	
	HC′O	117.5	117.6	117.8	118.2	
	H′C′O	112.5	112.9	113.5	113.8	
CH_3OCH (C_1)	C′H	1.116	1.113	1.107	1.107	
	C′O	1.310	1.299	1.299	1.295	
	CO	1.449	1.444	1.445	1.437	
	COC′	115.2	115.2	115.4	115.6	
	OC′H′	101.4	101.6	101.9	102.1	

[a] Bond distances in Å, bond angles in deg. [b] Reference 17. [c] Reference 18. [d] Reference 19. [e] Reference 20. [f] Reference 21. [g] Reference 22.

and eq 10 a 1,1-H_2 molecular elimination, both involve three-center transition states. It is interesting to note that the net reaction of eqs 2 and 3 is kinetically indistinguishable from the primary decomposition pathway shown in eq 8.

Computational Details

Equilibrium geometries and transition state structures were obtained using the second-order Møller−Plesset perturbation level of theory (MP2)[10] and the following basis sets: 6-31G(d),[11] 6-311G(d,p),[12] 6-311G(2d,2p), 6-311G(2df,2p). The latter two basis sets are derived from the 6-311G(d,p) basis set by adding a second set of (five) d-type polarization functions on the carbon and oxygen atoms and a second set of p-type polarization functions on the hydrogen atoms. The 6-311G(2df,2p) basis set also includes a set of (seven) f-type polarization functions on the carbon and oxygen atoms. The MP2 calculations included full electron correlation (i.e., the frozen-core approximation was not used).

Single-point calculations were performed with the coupled-cluster, including single, double, and perturbative triple excitations (CCSD(T))[13] methods as well as with the spin-projected, fourth-order Møller−Plesset perturbation method (PMP4) using the 6-311G(2df,2p) basis set. Additional CCSD(T) calculations were performed using the expanded 6-311++G(3df,3dp) basis set, which includes two additional sets of diffuse functions and an additional set of (five) d-type polarization functions on all atoms. All single-point calculations used the geometries obtained at the MP2/6-311G(2df,2p) level of theory. The frozen-core approximation was employed for the CCSD(T) and PMP4 calculations.

Vibrational frequencies and zero-point energies were obtained from analytical second derivatives calculated at the MP2/6-31G(d) level of theory using the MP2/6-31G(d) optimized geometries. Vibrational frequency calculations were also carried out at the MP2/6-311G(2d,2p) level using the MP2/6-311G(2d,2p) optimized geometries. All reactants and products were identified as true minima on the potential energy surface by the absence of any negative eigenvalues in the Hessian matrix. All transition-state structures showed a single negative eigenvalue in the Hessian matrix. The MP2/6-31G(d)-derived zero-point energies were scaled by a factor of 0.9646 as suggested by Radom et al.[14]

All molecular orbital calculations were performed with either the GAUSSIAN 92/DFT[15] or GAUSSIAN 94[16] programs.

Results and Discussion

Geometries. The optimized equilibrium geometries obtained at the various levels of theory for all reactants and products are listed in Table 1. The optimized structures obtained for the

TABLE 2: Selected Geometrical Parameters for Transition States[a]

		MP2/			
transition state	coordinate	6-31G(d)	6-311G(d,p)	6-311G(2d,2p)	6-311G(2df,2p)
$[CH_3OH + CH_2]$ (C_1)	C′O	1.758	1.719	1.730	1.703
	CO	1.443	1.435	1.437	1.431
	OH	1.023	1.018	1.023	1.018
	C′H′	1.096	1.098	1.091	1.090
	C′H	1.099	1.096	1.087	1.090
	COC′	109.8	109.8	109.0	109.5
	C′OH	63.4	62.0	61.0	63.1
	COH	108.6	108.0	108.5	108.9
	HC′H′	106.3	106.8	107.0	107.1
	HC′O	99.9	100.7	100.4	100.7
	H′C′O	97.3	98.4	98.3	98.5
$[CH_4 + CH_2O]$ (C_s)	CO	1.342	1.329	1.329	1.322
	CH	1.190	1.196	1.197	1.199
	C′H	1.800	1.778	1.765	1.762
	CH′	1.100	1.100	1.093	1.094
	C′H″	1.075	1.072	1.066	1.067
	C′H‴	1.092	1.094	1.086	1.086
	OCH	104.9	104.5	104.5	104.5
	CHC′	115.2	114.2	114.3	113.7
	H′CH′	113.5	113.8	114.2	114.1
	H″C′H″	123.0	124.3	124.3	124.7
	H″C′H‴	115.5	116.1	116.2	116.1
$[CH_3OCH + H_2]$ (C_1)	CO	1.436	1.430	1.433	1.426
	C′O	1.337	1.327	1.327	1.322
	C′H′	1.101	1.104	1.097	1.098
	C′H″	1.298	1.345	1.349	1.361
	H″H‴	0.895	0.863	0.861	0.854
	H′H‴	2.004	1.972	1.975	1.975
	COC′	113.2	113.1	113.5	113.7
	OC′H′	106.8	106.7	107.0	107.0
	OC′H″	114.8	114.4	114.3	114.1
	H′C′H″	105.1	103.0	102.6	102.3
	C′H″H‴	108.4	106.5	106.9	106.7

[a] Bond distances in Å, bond angles in deg.

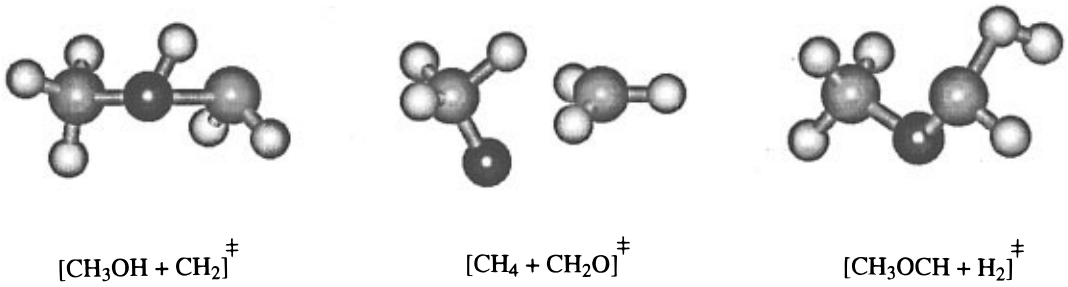

Figure 1. MP2/6-311G(2df,2p) optimized geometries for the transition states for the dissociation of dimethyl ether.

three transition states are listed in Table 2, and the MP2/6-311G-(2df,2p) optimized structures are depicted in Figure 1. The corresponding total energies are listed in Table 3.

In general, the calculated equilibrium bond lengths decrease slightly as the basis set is expanded from 6-31G(d) to 6-311G-(2df,2p). However, the largest change in C−H bond length is 0.009 Å, and the largest change in either C−O or O−H bond length is 0.018 Å. The changes in bond angles are also relatively small—the largest change is 1.3°. This suggests that the geometries are relatively well converged at the MP2 level and additional expansion of the basis set will only produce minor changes in the equilibrium geometries.

For those molecules where there is an experimentally determined geometry available (see Table 1), reasonably good agreement between the experimental and calculated geometries is achieved. For example, at the MP2/6-311G(2df,2p) level, the largest differences between calculated and experimental bond lengths and bond angles are 0.017 Å (CH_2O (C−H)) and 1.4° (CH_3OH (HCO)), respectively.

Similar trends are also observed for the transition states although the largest changes in bond lengths and bond angles are slightly larger (0.063 Å and 2.8°, respectively). The MP2/6-311G(2df,2p) optimized geometries for the $[CH_3OH + CH_2]$ and $[CH_3OCH + H_2]$ transition states suggest that these two transition states occur late on the potential energy surface as the optimized geometries resemble the products of the reactions. For example, for the $[CH_3OH + CH_2]$ transition state, the optimized C−O and O−H bond lengths (1.431 and 1.018 Å, respectively) differ from the optimized C−O and O−H bond lengths for methanol by only 0.019 and 0.062 Å, respectively. For the $[CH_3OCH + H_2]$ transition state, the optimized C−O and H−H bond lengths (1.426, 1.322, and 0.854 Å, respectively) differ from the optimized C−O and H−H bond lengths for CH_3-OCH and H_2 by only 0.011, 0.027, and 0.119 Å, respectively.

For the $[CH_4 + CH_2O]$ transition state, the C−O bond is virtually completely broken (2.263 Å) whereas the C−H bond to produce methane (1.762 Å) is only partially formed. This suggests that this transition state contains a significant amount

TABLE 3: Total Energies for Reactants, Products, and Transition States[a]

	MP2/				PMP4/[b]	CCSD(T)/[b]	
molecule	6-31G(d)	6-311G(d,p)	6-311G(2d,2p)	6-311G(2df,2p)	6-311G(2df,2p)	6-311G(2df,2p)	6-311++G(3df,3pd)
				Reactants and Products			
H	−0.498 23	−0.499 81	−0.499 81	−0.499 81	−0.499 81	−0.499 81	−0.499 82
H_2	−1.144 14	−1.160 27	−1.162 76	−1.162 76	−1.170 21	−1.170 80	−1.172 51
CH_2	−38.970 24	−39.022 38	−39.034 65	−39.044 05	−39.051 46	−39.055 40	−39.061 89
CH_3	−39.669 63	−39.725 67	−39.739 07	−39.749 29	−39.754 41	−39.754 52	−39.761 23
CH_4	−40.333 49	−40.398 04	−40.414 07	−40.425 04	−40.430 53	−40.431 01	−40.438 13
CH_2O	−114.167 73	−114.272 43	−114.303 09	−114.336 39	−114.324 76	−114.321 97	−114.336 23
CH_3O	−114.686 20	−114.797 97	−114.830 12	−114.861 68	−114.860 39	−114.860 76	−114.876 96
CH_3OH	−115.346 10	−115.474 07	−115.510 10	−115.542 82	−115.535 47	−115.534 68	−115.554 86
CH_3OCH	−153.239 29	−153.382 28	−153.425 57	−153.471 15	−153.462 64	−153.461 74	−153.481 98
CH_3OCH_2	−153.853 27	−154.013 30	−154.059 08	−154.105 64	−154.096 58	−154.095 40	−154.117 15
CH_3OCH_3	−154.504 62	−154.672 43	−154.720 35	−154.767 29	−154.758 69	−154.757 36	−154.780 14
				Transition States			
$[CH_3OH + CH_2]$	−154.347 65	−154.528 68	−154.577 29	−154.622 17	−154.617 43	−154.616 18	−154.640 82
$[CH_4 + CH_2O]$	−154.338 20	−154.510 89	−154.562 72	−154.606 59	−154.611 01	−154.607 32	−154.630 74
$[CH_3OCH + H_2]$	−154.354 81	−154.521 39	−154.568 43	−154.615 01	−154.612 86	−154.612 51	−154.635 46

[a] Total energies in au. [b] Single-point calculations using the MP2/6-311G(2df,2p) optimized geometries.

TABLE 4: Vibrational Frequencies and Zero-Point Energies for Reactants, Products, and Transition States[a,b]

molecule	frequencies[c]	zero-point energy[d]
H_2	4534	6.3
CH_2	3472, 3251, 1191	10.9
CH_3	3402′, 3214, 1482′, 416	18.5
CH_4	3244″, 3107, 1626′, 1415″	28.0
CH_2O	3086, 3014, 1791, 1584, 1296, 1210	16.5
CH_3O	3165, 3133, 3048, 1584, 1486, 1467, 1142, 1003, 837	23.3
CH_3OH	3786, 3222, 3143, 3076, 1580, 1567, 1541, 1417, 1206, 1115, 1086, 351	31.8
CH_3OCH	3257, 3248, 3133, 2929, 1557, 1550, 1513, 1458, 1396, 1221, 1200, 957, 755, 529, 159	34.3
CH_3OCH_2	3340, 3235, 3179, 3170, 3087, 1569, 1556, 1553, 1512, 1317, 1288, 1207, 1172, 995, 786, 441, 311, 182	41.2
CH_3OCH_3	3217, 3216, 3122, 3117, 3058, 3050, 1583, 1567, 1559, 1549, 1547, 1512, 1302, 1241, 1231, 1196, 1156, 975, 428, 269, 223	49.8
$[CH_3OH + CH_2]$	3246, 3225, 3181, 3123, 3082, 3042, 1563, 1557, 1515, 1492, 1405, 1230, 1188, 1150, 1089, 1007, 459, 325, 266, 223, 961*i*	46.0
$[CH_4 + CH_2O]$	3455, 3334, 3155, 3129, 3048, 2017, 1610, 1595, 1565, 1458, 1421, 1247, 1199, 1135, 876, 835, 694, 529, 399, 334, 962*i*	45.6
$[CH_3OCH + H_2]$	3248, 3210, 3110, 3098, 2395, 1609, 1562, 1548, 1523, 1451, 1325, 1266, 1208, 1163, 990, 950, 674, 475, 262, 142, 1235*i*	43.0

[a] Calculated at the MP2/6-31G(d) level. [b] Frequencies in cm^{-1}, zero-point energies in kcal/mol. [c] Single prime indicates double degeneracy; double prime indicates triple degeneracy. [d] Scaled by a factor of 0.9646 (see ref 14).

of ionic character. Indeed, the Mullikin population analysis for this transition state shows high negative charge density on the oxygen atom (−0.61) and high positive charge densities on both carbon atoms (+0.21 and +0.40).

Vibrational Frequencies. The calculated (i.e., MP2/6-31G(d)) vibrational frequencies and scaled[14] zero-point energy corrections for all structures are presented in Table 4. The calculated frequencies are expected to be overestimated by about 6−8% compared to the exact harmonic frequencies. A scaling factor of 0.9427 has been suggested[14] for MP2/6-31G(d)-derived frequencies.

The vibrational frequencies for the transition-state structures are each characterized by one imaginary frequency. The imaginary frequency for the 1,2-elimination of CH_4 is calculated to be 962*i*. The nature of the transition vector for this normal mode suggests that motion consists of an H-atom transfer from the CH_3 group mixed with COC bending. The imaginary frequency (1235*i*) for the 1,1-H_2 elimination transition state consists mainly of CH_2 bending, which brings the two hydrogens together while the CH bonds elongate in the process of forming H_2. The imaginary frequency (961*i*) for the three-center elimination of CH_2 corresponds to a 1,2-H shift mixed with CH_2 rotation.

Enthalpies of Decomposition Reactions and Barrier Heights. The calculated enthalpies of reaction for the various decomposition pathways for dimethyl ether, corrected for zero-point energy differences, are listed in Table 5.

Using the known, experimentally determined values for the heats of formation of dimethyl ether (−39.7 ± 2 kcal/mol[23]), CH_4 (−15.99 ± 0.08 kcal/mol[24]), CH_2O (−26.78 ± 1.5 kcal/mol[24]), and CH_3OCH_2 (4.2 ± 2 kcal/mol[25]), the reliability of the calculated enthalpies of reaction for the various decomposition pathways for dimethyl ether can be estimated. Using these values, $\Delta H°$ for the reaction $CH_3OCH_3 \rightarrow CH_4 + CH_2O$ is estimated to be −3.1 ± 1.8 kcal/mol. The calculated values for this reaction all fall within the error bounds of this estimate, but the MP2/6-31G(d), MP2/6-311G(2d,2p) and PMP4/6-311G(2df,2p) calculations provide the best agreement differing by only 0.1, 0.2 and 0.1 kcal/mol, respectively. For the reaction $CH_3OCH_3 \rightarrow CH_3 + CH_3O$, $\Delta H°$ for the C−O bond fission process has been experimentally measured to be 81.1 kcal/mol.[3] All of the MP2 calculations for this reaction predict enthalpies that are too high (by 4.3−9.0 kcal/mol) compared with the experimental value. However, the PMP4 and CCSD(T) calculations fare much better—$\Delta H°$ is predicted to be 82.3 and 81.1 kcal/mol, respectively, in much better agreement with the experimentally determined value.

Similar agreement exists between the experimentally estimated $\Delta H°$ and the calculated reaction enthalpy for the CH_3-

TABLE 5: Enthalpies of Decomposition Reactions[a]

	$CH_3OCH_3 \rightarrow$				
level	$CH_4 + CH_2O$	$CH_3OCH + H_2$	$CH_3 + CH_3O$	$CH_3OCH_2 + H$	$CH_3OH + CH_2$
MP2/6-31G(d)//MP2/6-31G(d)	−3.2	66.8	85.4	87.5	111.0
MP2/6-311G(d,p)//MP2/6-311G(d,p)	−4.1	72.3	85.4	91.4	103.3
MP2/6-311G(2d,2p)//MP2/6-311G(2d,2p)	−3.3	73.6	86.9	92.7	103.1
MP2/6-311G(2df,2p)//MP2/6-311G(2df,2p)	−1.6	74.5	90.1	93.0	106.1
	Using MP2/6-311G(2df,2p) Geometries				
PMP4/6-311G(2df,2p)	−3.2	69.8	82.3	93.2	100.7
CCSD(T)/6-311G(2df,2p)	−2.6	69.1	81.2	93.2	97.9
CCSD(T)/6-311++G(3df,3pd)	−1.7	69.6	81.1	93.8	95.4

[a] Corrected for zero-point energy differences; in kcal/mol.

TABLE 6: Barrier Heights[a]

	$CH_3OCH_3 \rightarrow$				
level	$CH_4 + CH_2O$	$CH_3OCH + H_2$	$CH_3 + CH_3O$	$CH_3OCH_2 + H$	$CH_3OH + CH_2$
MP2/6-31G(d)//MP2/6-31G(d)	100.2	87.2	85.4	87.5	94.7
MP2/6-311G(d,p)//MP2/6-311G(d,p)	97.2	88.0	85.4	91.4	86.4
MP2/6-311G(2d,2p)//MP2/6-311G(2d,2p)	94.7	88.5	86.9	92.7	86.0
MP2/6-311G(2df,2p)//MP2/6-311G(2df,2p)	96.6	88.8	90.1	93.0	87.3
	Using MP2/6-311G(2df,2p) Geometries				
PMP4/6-311G(2df,2p)	88.5	84.7	82.3	93.2	84.8
CCSD(T)/6-311G(2df,2p)	90.0	84.1	81.2	93.2	84.8
CCSD(T)/6-311++G(3df,3pd)	89.5	84.0	81.1	93.8	83.6
exptl			81.1[b]	95.5[c]	

[a] Corrected for zero-point energy differences; in kcal/mol. [b] Reference 3. [c] Reference 6.

$OCH_3 \rightarrow CH_3OCH_2 + H$ reaction. The C−H bond fission process has been experimentally measured to be 95.5 kcal/mol.[6] Again, there is relatively poor agreement between the MP2 calculations and the experimental value—the MP2 calculations predict enthalpies of reaction that are too low by 2.5−8.0 kcal/mol. The PMP4 and CCSD(T) calculations also predict $\Delta H°$ values that are too low but only by 1.7−2.3 kcal/mol. The root-mean-square (rms) error between experimental and theoretical estimates at the CCSD(T)/6-311++G(3df,3pd)// MP2/6-311G-(2df,2p) level of theory is 1.3 kcal/mol. This is quite reasonable and suggests that the estimates of the energetics for the other pathways should be reliably well-predicted at this level of theory.

At the CCSD(T)/6-311++G(3df,3pd) level, the five decomposition pathways (i.e., 1,2-elimination of CH_4, 1,1-elimination of H_2, C−O bond fission, C−H bond fission, and 1,2-H shift to yield CH_2 and CH_3OH) appear thermodynamically competitive. The predicted enthalpies of reaction for these five reactions are −1.7, 69.6, 81.1, 93.8, and 95.4 kcal/mol, respectively. However, the energetic ordering of these five thermodynamically competitive pathways changes considerably when the kinetics of these reactions are considered.

Table 6 lists the calculated barrier heights for the decomposition processes. The activation barrier for the 1,1-elimination of H_2 is estimated to be 84.0 kcal/mol. This activation barrier is ca. 2.9 kcal/mol greater than the activation barrier for C−O bond fission—the lowest energy decomposition process. These data suggests that 1,1-elimination of H_2 is potentially a competitive channel. Moreover, the 1,2-elimination of CH_4 (89.5 kcal/mol) may also be competitive. Thermodynamically, the 1,2-elimination of CH_4 is the most favorable process; however, kinetically, it has an activation barrier that is 8.4 kcal/mol larger than the C−O bond fission process. Under experimental conditions of high excitation energy characteristic in combustion processes, this channel could become kinetically competitive with the C−O bond fission process. In such a case there would be two kinetically distinct processes occurring to yield very similar products: (1) $CH_4 + CH_2O$ from the 1,2-elimination reaction and (2) $CH_4 + CH_2O$ resulting from the chain propagation reaction of CH_3 radicals produced from C−O bond fission of dimethyl ether via reactions 2 and 3.

The estimated activation barrier for the 1,2-H shift process to yield CH_2 and CH_3OH at the CCSD(T)/6-311++G(3df,3pd)//MP2/6-311G(2df,2p) level falls below the enthalpy for the products of this reaction by 11.8 kcal/mol. This suggests that there is no barrier for the reverse reaction. Calculations at several points along the reaction path connecting the reactant and transition state showed no maximum, only a smoothly increasing energy profile. Therefore, an estimate of the activation barrier for this process is given by the computed enthalpy of 95.4 kcal/mol. This is predicted to be the least favored process being 1.6 kcal/mol above the C−H bond fission process.

Dimethyl ether is being considered as an alternative diesel fuel by Topsie and Amoco. Consequently, it is important to identify and to understand all of the possible pathways accessible in the combustion process. The present calculations suggest that in addition to the two previously observed processes, i.e., C−O and C−H bond fission, 1,1-elimination of H_2 and 1,2-elimination of CH_4 are also competitive channels.

Acknowledgment. We thank the Purdue University Computing Center and the Pittsburgh Supercomputing Center for ample provision of computing resources, which has made this work possible. J.S.F. thanks M. M. Maricq for helpful discussions.

References and Notes

(1) Askey, P. J.; Hinshelwood, C. N. *Proc. R. Soc. London* **1927**, *A115*, 215.
(2) Leifer, E.; Urey, H. C. *J. Am. Chem. Soc.* **1942**, *64*, 994.
(3) Benson, S. W. *J. Chem. Phys.* **1956**, 25, 27.
(4) Benson, S. W.; Jain, D. V. S. *J. Chem. Phys.* **1959**, 31, 1008.
(5) Marcus, R. A.; Darwent, B. de B.; Steacie, E. W. R. *J. Chem. Phys.* **1948**, 16, 987.
(6) Loucks, L. F.; Laidles, K. J. *Can. J. Chem.* **1967**, *45*, 2763.

(7) Takezaki, Y.; Mori, S.; Kawasaki, H. *Bull. Chem. Soc. Jpn.* **1966**, *39*, 1643.
(8) Pottie, R. F.; Harrison, A. G.; Lossing, F. P. *Can. J. Chem.* **1961**, *39*, 102.
(9) Kutschke, K. O.; Willis, C.; Hackett, P. A. *J. Photochem.* **1983**, 21, 207.
(10) Kirshnan, R.; Pople, J. A. *Int. J. Quantum Chem. Symp.* **1980**, 14, 91.
(11) Harihavan, P. C.; Pople, J. A. *Theor. Chim. Acta* **1973**, 28, 213.
(12) Frand, M. M.; Pieto, W. J.; Hehre, W. J.; Binkley, J. S.; Gordon, M. S.; DeFrees, D. J.; Pople, J. A. *J. Chem. Phys.* **1982**, 77, 3654.
(13) (a) Purvis, G. D., III; Bartlett, R. J. *J. Chem. Phys.* **1982**, 76, 1910. (b) Lee, T. J.; Rendell, A. P. *J. Chem. Phys.* **1991**, 69, 399.
(14) Pople, J. A.; Scott, A. P.; Wong, M. W.; Radom, L. *Isr. J. Chem.* **1990**, 33, 345.
(15) Frisch, M. J.; Trucks, G. W.; Head-Gordon, M.; Gill, P. M. W.; Wong, M. W.; Foresman, J. B.; Johnson, B. G.; Schlegel, H. B.; Robb, M. A.; Replogle, E. S.; Gomperts, R.; Andres, J. L.; Raghavachari, K.; Binkley, J. S.; Gonzalez, C.; Martin, R. L.; Fox, D. J.; Defrees, D. J.; Baker, J.; Stewart, J. J. P.; Pople, J. A. *Gaussian 92*, Revision D.2; Gaussian, Inc.: Pittsburgh, PA, 1992.
(16) Frisch, M. J.; Trucks, G. W.; Schlegel, H. B.; Gill, P. M. W.; Johnson, B. G.; Robb, M. A.; Cheeseman, J. R.; Keith, T.; Petersson, G. A.; Montgomery, J. A.; Raghavachari, K.; Al-Laham, M. A.; Zakrzewski, V. G.; Ortiz, J. V.; Foresman, J. B.; Peng, C. Y.; Ayala, P. Y.; Chen, W.; Wong, M. W.; Andres, J. L.; Replogle, E. S.; Gomperts, R.; Martin, R. L.; Fox, D. J.; Binkley, J. S.; Defrees, D. J.; Baker, J.; Stewart, J. P.; Head-Gordon, M.; Gonzales, C.; Pople, J. A. *Gaussian 94*, Revision B.3; Gaussian, Inc.: Pittsburgh, PA, 1995.
(17) Kolos, W.; Wolniewicz, L. *J. Chem. Phys.* **1968**, 49, 404.
(18) Herzberg, G. *Proc. R. Soc. London* **1961**, *A262*, 291.
(19) (a) Tarrago, G.; Dang-Nhu, M.; Poussigue, G. *J. Mol. Spectrosc.* **1974**, 49, 322. (b) Olson, W. B. *J. Mol. Spectrosc.* **1972**, 43, 190.
(20) (a) Takagi, K.; Oka, T. *J. Phys. Soc. Jpn.* **1963**, 18, 1174. (b) Oka, T. *J. Phys. Soc. Jpn.* **1960**, 15, 2274.
(21) (a) Lees, R. M.; Baker, J. G. *J. Chem. Phys.* **1968**, 48, 5299. (b) Kwan, Y. Y.; Dennison, D. M. *J. Mol. Spectrosc.* **1972**, 43, 291. (c) Gerry, M. C. L.; Lees, R. M. *J. Mol. Spectrosc.* **1976**, 61, 231.
(22) Blukis, U.; Kasai, P. H.; Myers, R. J. *J. Chem. Phys.* **1963**, 38, 2753.
(23) Lias, S. G.; Bartmess, E.; Liebman, J. F.; Holmes, J. L.; Levin, R. D.; Mallard, W. G. *J. Phys. Chem. Ref. Data* **1988**, 17 (Suppl. 1).
(24) Chase, M. W., Jr.; Davies, C. A.; Downey, J. R., Jr.; Frurip, D. J.; McDonald, R. A.; Syverud, A. N., *J. Phys. Chem. Ref. Data* **1985**, 14 (Supplement 1).
(25) Good, D. A.; Francisco, J. S. *Chem. Phys. Lett.* **1997**, 266, 512.